

# Model-Free Analysis of Neutron Reflectivity Data from Polymer Thin Films with the Simulated Annealing Technique

K. Kunz, J. Reiter,<sup>†</sup> A. Götzelmann, and M. Stamm\*

Max-Planck-Institut für Polymerforschung, Postfach 55021 Mainz, Germany

Received December 17, 1992; Revised Manuscript Received May 4, 1993

**ABSTRACT:** Neutron reflectivity is widely accepted as a technique to investigate interfacial properties with excellent resolution in many areas of polymer science. The use of simulated annealing procedures in connection with the matrix method and a matrix-tree algorithm is proposed to obtain a model-free fit of the scattering density profile from a given experimental neutron reflectivity curve. Due to the ill-defined nature of the phaseless Fourier transform problem, multiple minima and ambiguities exist. Simulated annealing procedures make it possible to overcome barriers and local minima during a fit since with a certain probability also those variations are accepted during the minimization procedure which do not improve the fit. To obtain physically meaningful solutions close to the global minimum, additional conditions have to be introduced and a reasonable starting profile has to be given. The potential of the technique is demonstrated by the analysis of theoretical model curves as well as experimental neutron reflectivity data. For the enrichment of components at interfaces, the interdiffusion between polymer films, and the development of surface-induced order in diblock copolymers, the method proves to reveal relevant features while specific details of the profiles are in some cases difficult to resolve.

## 1. Introduction

Neutron reflectivity is a technique with unique possibilities for the investigation of polymer surfaces and interfaces.<sup>1,2</sup> This is to a large extent due to the large contrast which can generally be generated between components by deuteration of one species as well as to the excellent depth resolution of the technique.<sup>3</sup> Thus e.g. the interface width between two polymer films can be determined with subnanometer resolution and in addition the scattering density profile may be resolved. Therefore the technique has been applied to various problems connected with interfacial properties of polymers including, for instance, the initial stages of interdiffusion between two polymer films,<sup>4,5</sup> the surface enrichment of components in a polymer blend,<sup>6</sup> or the surface induced order of blockcopolymers in a thin film.<sup>7</sup>

In the analysis of neutron reflectivity data from polymeric film systems, one is faced with the problem to obtain a reliable scattering density profile which is physically meaningful and consistent with already known parameters of the system. Those parameters could be for instance layer thicknesses, mean densities, or interfacial roughnesses. A solution is generally not unique because of the phase problem, and many local minima for the deviation between experimental data and fit may exist. One usually tries to construct a model profile on the basis of the knowledge about the systems and to refine some (or all) parameters of the model. This procedure is thus closely connected to a particular model scattering density profile which one might guess from theory or intuition, but relevant features of the solution might be missing. In particular for more complicated problems which could be already a thin film of a polymer blend with different components on a substrate or a double layer system of two thin polymer films with interdiffusion and surface enrichment, it is sometimes difficult to obtain a good guess for an analytic form of the scattering density distribution. It sometimes turns out that the reflectivity curve can be quite sensitive on particular details of the model and various parameters could have a compensating effect on

the reflectivity fit. There is, of course, no general unique solution to this problem but the use of model-free fits can help to understand relevant features of the profile and might give a hint to, e.g., a specific interface enrichment or density distribution which might not be included in a simple model. Here we propose the use of the simulated annealing algorithm<sup>8,9</sup> in connection with the matrix technique<sup>10,11</sup> for the calculation of neutron reflection curves to generate a model-free fit of a scattering density profile to a given experimental neutron reflectivity curve. Because of the lack of phase information, we are, of course, still faced with the general problem to obtain a unique solution from a measured reflectivity curve which to some extent can be solved using as much additional information on the investigated sample as possible.

There are principally four ways of data analysis used up to now: (i) model fitting mostly in connection with the matrix technique<sup>10,11</sup> or recursion relations;<sup>12,13</sup> (ii) approximation techniques which in specific cases allow the direct estimate of certain parameters from the measured reflectivity curve;<sup>10,14</sup> (iii) inversion techniques where the direct inversion of reflectivity data into scattering density profiles is tried;<sup>10</sup> (iv) model-free fitting of reflectivity data again based on the matrix technique or approximation formulas. We have already mentioned problems connected with model fitting, approach i. Approximation techniques, approach ii, are based on kinematic scattering theory and neglect multiple reflections.<sup>10,14</sup> They are best suited for weakly reflecting smooth interfaces far away from the total reflection region. In this limit analytical expressions between reflected amplitude and scattering density profile can be derived<sup>15-17</sup> which may be used to obtain specific parameters of the profile by suitable plots of the reflectivity data.<sup>18,19</sup>

The most direct way of data analysis would be, of course, the direct inversion of the reflectivity curve into a scattering density profile, approach iii. This is, however generally not possible since phases are not known without further information. The first problem one is facing when one tries to invert experimental data is the lack of general analytic expressions for the relation between scattering density and reflectivity curve. Only in simple cases<sup>10</sup> such relations exist and only recently a more general relation is suggested.<sup>17,20</sup> For most practical cases one has to use

\* To whom correspondence should be addressed.

<sup>†</sup> Present address: École Nationale Supérieure des Mines des Paris, Sophia Antipolis, 06560 Valbonne, France.

either approximation formulas or numerical techniques to determine the reflectivity from a given density profile. Based on approximation formulas one obtains a quantity analogous to the Patterson function by direct Fourier transform of experimental reflectivity data.<sup>21,22</sup> Similar to normal scattering theory it is not easy to interpret the Patterson function in terms of the actual underlying density profile, but techniques similarly known in scattering theory may be also adopted to the reflectivity problem. Thus contrast variation by isotopic substitution,<sup>18</sup> anomalous scattering utilizing synchrotron radiation,<sup>23,24</sup> or ferroelectric substrates in combination with polarized neutrons<sup>25</sup> help to solve the phase problem. A combination of indirect Fourier transformation and square-root deconvolution<sup>26</sup> is shown to reveal the scattering density profile under certain approximations, and other approaches for the solution of the inversion problem are discussed.<sup>17,20,27</sup> They all have in common that approximation formulas are used which are rigorously valid only for smooth weakly reflecting profiles away from the total reflection edge, even if they have been shown to give reliable approximations over a large angular range if used with some further modifications.<sup>17,28</sup> Inversion techniques are thus mostly used as supplementary techniques to determine significant features of the profile.

As a model-free fitting technique based on the matrix method (approach iv) recently the maximum entropy algorithm is applied to the analysis of reflectivity data.<sup>29</sup> The profile is divided into a certain number of layers and starting from a reasonable initial profile entropy is used as a regularising function for the fit of the reflectivity curve by variation of the step height in the layer profile during the computations. Limitations of the technique are discussed and the importance of the inclusion of known parameters into the fit is emphasized to obtain a reliable scattering density profile. Calculations turn out to be very computer time consuming.

We propose another approach of model-free fitting of reflectivity data based on the simulated annealing algorithm<sup>8</sup> in connection with the matrix technique. Simulated annealing is a general fitting procedure which allows to overcome local minima during the fit. It thus helps to find the global minimum in a multimimum problem which generally exists for the solution of the phase problem in a reflectivity experiment. It will become evident that the simulated annealing algorithm will give useful hints for possible solutions while the unambiguity of the solutions can only be removed by additional information about the sample. Simulated annealing has successfully been used in different areas including physics, chemistry, biology, and engineering.<sup>30,31</sup> Recent applications to quite similar problems in crystallography have been reviewed.<sup>32</sup> We will first shortly describe the technique as it is applied to reflectivity data and then discuss on the basis of some examples the potential and limitations of this approach for the investigation of polymer interfaces by reflectivity techniques.

## 2. Simulated Annealing

For the calculation of reflectivity curves from a given density profile for comparison with experimental data, we use the matrix technique.<sup>10,11</sup> The generally smooth profile which might be given in the form of an analytical function has to be approximated by  $N$  discrete layers or step functions of width  $d_i$  and indices of refraction  $n_i$ ,  $1 \leq i \leq N$ . The indices of refraction  $n_i$  are connected to the

scattering densities  $\rho_i \bar{b}_i$  for neutrons<sup>10</sup>

$$n_i = 1 - \frac{\lambda^2}{2\pi} \rho_i \bar{b}_i \quad (1)$$

where  $\lambda$  is the neutron wavelength,  $\rho_i$  the number density of layer  $i$ , and  $\bar{b}_i$  the mean neutron scattering length of scattering particles in this layer. The matrix technique is an "exact" way to calculate reflectivity curves from density profiles provided the profile is approximated by a sufficient number of steps. Sufficient in that sense means that the step size is adapted to the experimental resolution which is given by the magnitude of the maximal measured wave vector,  $k_{\max} = (2\pi/\lambda) \sin \theta_{\max}$ .  $\lambda$  is the neutron wavelength and  $\theta_{\max}$  the largest measured angle. Details of the density profile which are smaller than  $\pi/k_{\max}$  cannot be resolved given the specific experimental data. The step widths  $d_i$  for the approximation of the model profile can thus be adapted in a suitable way.

The indices of refraction of step 0 and  $N + 1$  are given as boundary conditions and are, for instance, the values of air or glass. The matrix for step function  $i$  is for angle  $\theta$

$$M_i = \begin{bmatrix} \cos(k_i d_i) & k_i^{-1} \sin(k_i d_i) \\ -k_i \sin(k_i d_i) & \cos(k_i d_i) \end{bmatrix} \quad (2)$$

where  $k_i = 2\pi/\lambda(n_i^2 - n_0^2 \cos^2 \theta)^{0.5}$  holds. The product of the  $N$  noncommuting matrices is calculated

$$M = \begin{bmatrix} m_{11} & m_{21} \\ m_{21} & m_{22} \end{bmatrix} = M_N M_{N-1} \dots M_1 \quad (3)$$

and finally the reflectivity for angle  $\theta$  is obtained as

$$R = \frac{(k_0 k_{N+1} m_{12} + m_{21})^2 + (k_{N+1} m_{11} + k_0 m_{22})^2}{(k_0 k_{N+1} m_{12} - m_{21})^2 + (k_{N+1} m_{11} - k_0 m_{22})^2} \quad (4)$$

The fit proceeds by changing parameters in the analytical representation of the density profile such that the sum over different angles of the square of the difference between measured and calculated reflectivity is minimized. The reflectivity  $R$  is obtained experimentally from measured reflected intensities when the intensities are corrected for the primary beam intensity, geometrical effects, and background.

In this work we want to represent the density profile by an arbitrary set of discrete steps where the parameters for each step may be changed independently. In the fit, one of the  $N$  step functions is randomly selected and its index of refraction (and/or its width) is changed by a randomly chosen amount. The change is accepted if the sum of the least squares is smaller than (or equal to) the previous value (a further restriction is discussed below). If it is larger, the change is still accepted with some probability  $p$  smaller than unity; i.e., the larger the sum becomes, the smaller the probability of acceptance. With this method one can also escape from a local minimum (simulated annealing). The calculation of this probability is arbitrary and some examples will be discussed in chapter 3. One could, for instance, choose  $\exp(F_0 - F_n)/(F_n T)$ , where  $F_n$  is the new and  $F_0$  is the previous (old) sum of square deviations,  $F_n \geq F_0$ . The smaller  $1/T$ , the more likely one accepts parameters which yields a worse fit; i.e.,  $T$  is the analogue of temperature. Initially one chooses a large temperature  $T$  such that a bigger portion of parameter space is explored, and later when one optimizes preselected

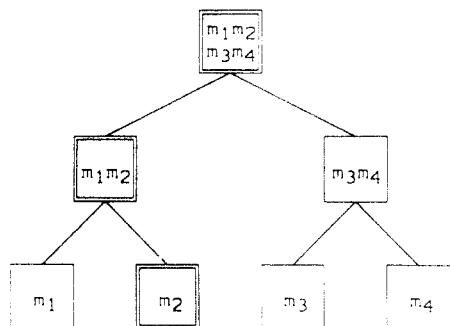


**Figure 1.** Binary tree of matrix products used for a fast calculation of reflectivity curves for four different matrices. If the second matrix is changed, it is multiplied with the first to obtain the new value for the first product in the second row which in turn is multiplied with its right neighbor to obtain the product of all four matrices. The matrices which are changed are marked by double lines.

parameters, a smaller  $T$  is chosen. In fact we use in the beginning of a fit sometimes a constant probability; i.e., if the new parameters set produced a worse fit than the old one, we accept it with a probability of, say, 5% (see also section 3). In later stages of the fit, a smaller probability is used.

Because of the limited experimental  $k$  range, the measured reflectivity usually does not contain information about short range oscillations ( $<3$  Å). Therefore one has to take additional precautions to avoid large short range oscillations in the data. One introduces a constraint on the simulated annealing procedure which does not permit an increase (decrease) in the index of refraction of a given step in the profile if (i) its index of refraction is larger (smaller) than both the index of refraction of its left and of its right neighbor and if (ii) in addition the maximum of the absolute value of the differences to its neighbors exceeds a chosen value. This is controlled by a constraint parameter  $C$  which limits the maximal variation of  $n$  as described above. Nevertheless the profile becomes rough if fitting proceeds for a longer time. Periodically one therefore smoothes it by simply weighting the index of refraction of step  $i$  with that of its neighbors; i.e. step  $n_i$  is replaced by  $(1/4)n_{i+1} + 1/2n_i + 1/4n_{i-1}$ . This is further discussed in section 3. The additional constraint and smoothing of the profile reduce significantly the number of independent variables and thus makes the fit only possible. Simulated annealing can of course also be used with profiles which are represented by analytical functions. The advantage of the method is, however, that one may obtain arbitrary shapes for the density profile unbiased from any model assumptions, but it may often be useful to combine free and model-based fitting.

In performing the computation, one has to keep in mind that matrix multiplication is noncommutative. If one changes only the parameters of one discrete step of the profile and consequently only one matrix, one still has to multiply all  $N$  matrices in the correct order. To minimize the computational effort, we have utilized a binary tree of matrix products, schematically shown in Figure 1. The number of steps  $N$  is chosen as a power of 2,  $N = 2^6$ . In the zeroth level,  $l = 0$ , the  $N (=1)$  corresponding matrices are stored. In the first level,  $l = 1$ ,  $N/2$  products of two matrices are stored, i.e., the  $j$ th matrix in the 1st ( $k$ th) level is the product of the  $(2j - 1)$ th and the  $(2j)$ th matrix in the zeroth ( $(k - 1)$ th) level. There are  $2^{l-k}$  matrices in the  $k$ th level and in the uppermost  $l$ th level the product of all  $N$  matrices is stored. If one changes the  $i$ th step, one replaces the  $i$ th matrix in the lowest level. Then one multiplies it with its appropriate neighbor to obtain a new

matrix for the next level. This new matrix is again multiplied with its appropriate neighbor to replace a matrix in the next upper level. By  $l$  matrix multiplications (instead of  $N - 1$ ) the whole tree is updated and in the uppermost level the new total product is obtained. The  $l$  old matrices have to be retained and are substituted back if the change is not accepted. Such a tree of products has to be stored for every  $k$  value where the reflectivity is calculated.

This procedure considerably accelerates computation since matrix multiplications are kept to the absolute minimum. Computation times for a complete simulated annealing fit do depend of course considerably on the number,  $N$ , of steps chosen as well as on the  $k$  range and accuracy in  $k$ , i.e. the number of  $k$  values in the fit. It does, however, also depend on the starting conditions and how many iterations and smoothing procedures are necessary during a fit. For a reasonably defined problem a computing time of typically 15–90 min may be expected (on a VAX station 3100) as will be discussed below. In the following we will demonstrate on some examples the possibilities, limitations, and problems of the technique using both calculated as well as experimental reflectivity data as a basis for the simulated annealing fits.

### 3. Results and Discussion

The technique of neutron reflectivity may be applied to various problems in the area of polymer thin films and interfaces.<sup>1–7</sup> Here we will discuss in particular the application of the simulated annealing algorithm to the detailed determination of the interface between two thin polymer films, the surface enrichment of one component in a blend of two polymers, and the measurement of surface induced order in diblock copolymers. Those examples are current areas of research and originate from the attempt to obtain “simple” and reliable fitting procedures to experimental neutron reflectivity data while keeping the input into the fits to a minimum. In many cases it is also not straightforward and easy to construct an analytical model which contains all relevant features of the system and gives a reliable fit to the data. This is in particular the case during the interdiffusion of different materials where profiles are asymmetric, a net mass flow across the interface occurs, and one component might be enriched at the surface, at least at later stages of interdiffusion. While the reflectivity technique is extremely sensitive on specific details of the profile where, e.g., the slope is large, it is very insensitive on others. In addition there are generally a large number of possible solutions given an experimental curve with limited  $k$  range and statistical errors. Simulated annealing procedures cannot overcome all of those problems but will give hints on possible solutions and on their reliability.

As a first example we will discuss the application of simulated annealing to the problem of the determination of the concentration or scattering density profile during initial stages of interdiffusion at the interface between two polymers. One of the components will be deuterated and one will start from a sharp interface in a double layer system of a protonated and deuterated film on a smooth substrate. Heating the sample above the glass transition temperature  $T_g$  of at least one of the components will start interdiffusion of components at the interface. For Fickian diffusion between identical materials, one can assume the formation of an error-function-type profile. For initial stages of interdiffusion at an interface between two polymers, however, significant deviations from a simple behavior are expected concerning both the time depen-

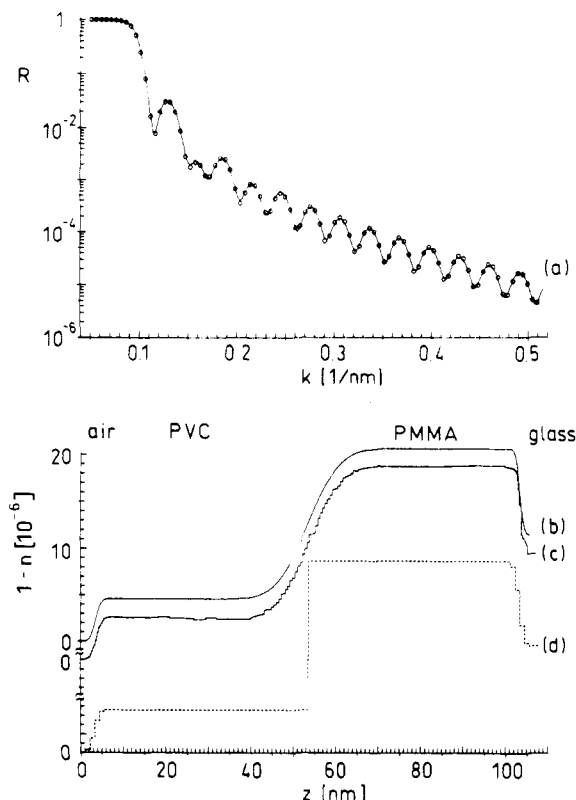


**Figure 2.** Simulated annealing fit of a calculated neutron reflectivity curve (a) of a layer of PVC ( $n = 1.46 \times 10^{-6}$ , thickness = 50 nm) on top of a layer of deuterated PMMA ( $n = 1.2065 \times 10^{-6}$ , thickness = 50 nm) on a glass substrate ( $n = 1.15 \times 10^{-6}$ ). The interfaces have error function form with a width of  $\sigma = 1$  nm for the polymer-air interface,  $\sigma = 6$  nm for the polymer-polymer interface, and  $\sigma = 0.8$  for the polymer-glass interface. There is excellent agreement between the "experimental" reflectivity curve (circles) and the fit (line). (b) In the upper part of the figure the model scattering length density profile expressed in  $(1-n)$  versus depth  $z$  is shown. It agrees very well with the fitted profile (c). The starting profile for the fit was a sharp step (dashed line, bottom).

dence of the interface width<sup>4,5</sup> as well as the form of the profile.<sup>33,34</sup> This is due to different time regimes of segmental motion across the interface as well as to possible distortions of the chain conformation or the enrichment of chain ends at the interface.<sup>35,36</sup>

In a first step the fitting procedure is tested using a model error function profile. A corresponding calculated reflectivity curve is taken as a basis for the simulated annealing fit. The profile of the index of refraction for such a layer system is shown in Figure 2. Also for the air-polymer and polymer-glass interfaces, error-function-type profiles have been assumed to simulate surface roughness which is typically of the order of 1 nm. The roughness of the air-polymer and air-glass interface and the thicknesses of the individual films can be determined from X-ray reflection experiments prior to neutron measurements,<sup>37</sup> and similarly also the mean scattering densities are known for the pure materials. This information is put into the starting profile shown in Figure 2d. The interface width and shape between the films is assumed to be unknown and approximated by a sharp step in the starting profile. The starting profile consisted of 32 layers of variable width.

The fit was done with a constant probability of  $p = 0.005$  to accept a worse  $F$  value and a constraint parameter  $C$  of  $0.25 \times 10^{-6}$ . The probability of changing the thickness  $d_i$  of a layer instead of changing its height (or  $n_i$  value) was 2%. The polymer-air interface was held

constant during the fit since small variations at this interface do not influence the reflectivity curve very much. To evaluate the quality of a fit, we use for the sum of the square deviations  $F_n$ , respectively, the form

$$F_n = \sum_i \frac{(R_{\text{exp}} - R_{\text{calc}})^2}{\min(R_{\text{exp}}, R_{\text{calc}})^2} \quad (5)$$

with  $R_{\text{exp}}$  being the experimental and  $R_{\text{calc}}$  the calculated reflectivity, respectively. This implies that we assume all values having the same relative error. Using a fit weighted with the statistical errors turns out to be not a reasonable procedure. Data in the low  $k$  range have very small statistical errors, but due to correction procedures for partial illumination of the sample, systematic errors are generally not negligible and difficult to specify. In addition usually the number of points in this range is chosen to be larger as compared to the wider  $k$  range, where experimental times to obtain reasonable statistics are much longer. Large  $k$  values prove, however, to be very important in the fit, since specific information of the profile, in particular details at a smaller length scale, is contained in data in this region. One therefore has to use a weighting of experimental points, which increases the importance of data points at large  $k$ .

After 100 iterations, where each iteration consists of 150 statistical variations of a particular layer parameter, one has to get rid of small scale oscillations which have no significant effect on the calculated reflectivity curve. This is done by averaging over neighboring points with statistical weights  $1/4$ ,  $1/2$ , and  $1/4$ . This smoothing procedure is applied twice to the whole profile except to the polymer-air interface. Subsequently the number of layers was doubled to 64 by linear interpolation. After further 30 iterations and another smoothing, the number of layers was doubled again. The result of the fit after another 30 iterations is again shown in Figure 2c. There is an excellent agreement between "experimental" and fitted reflectivity curves and the profiles agree very well, even if we did not input any information about the polymer-polymer interface, neither its functional form nor its width. The pathway of the fit has been largely determined by the starting profile already and starting with a more general profile might have generated a quite different fit. The complete fit described above took 30 min of computing time and gives a very reliable picture of the original profile which was assumed for the calculation of the "experimental" reflectivity curve. Slight variations in the starting profile do not significantly influence the result.

After this initial check one can proceed to actually measured neutron reflectivity curves. The system investigated consisted of a top layer of poly(vinyl chloride) (PVC,  $M_w = 39\,000$ ,  $T_g = 83^\circ\text{C}$ ) on a bottom layer of deuterated poly(methyl methacrylate) (PMMA,  $M_w = 75\,000$ ,  $T_g = 120.5^\circ\text{C}$ ) deposited on a float glass substrate. The sample used here was annealed between the glass transition temperatures of both polymers at  $T = 113^\circ\text{C}$ . In this temperature range the polymers are miscible,<sup>38</sup> while only PVC is above its  $T_g$  and mobile.

Parts a and b of Figure 3 show the measured neutron reflectivity curves after annealing of the sample for 3.5 and 7.5 h. The starting profiles, Figure 3d,f, consist of two layers of the two polymers on a glass substrate. The polymer-polymer interface after interdiffusion was modeled simply with a straight line. In order to take into account that the contact of the glass and the polymer is not perfect, the glass-polymer interface was represented by a superposition of error-function and exponential

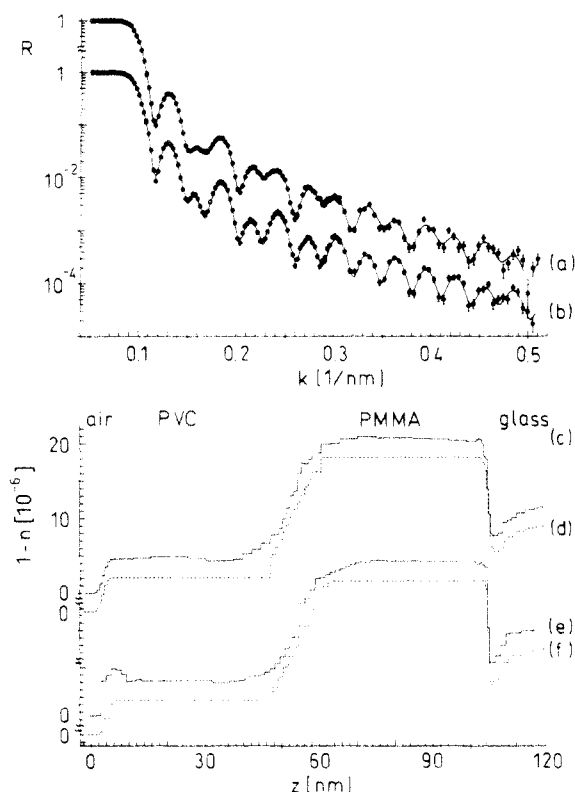


**Figure 3.** Simulated annealing fits to experimental neutron reflectivity curves of the system PVC on top of a layer of deuterated PMMA on a glass substrate. Samples are annealed between the glass transition temperatures of both polymers at 113 °C for (a) 3.5 h and (b) 7.5 h. The agreement between experimental (dots) and fitted reflectivities (broken lines) is well within experimental errors. The scattering density profiles expressed in  $(1 - n)$  are shown in the lower part of the figure. For the starting profiles (curves d and f) the interface between the two polymer layers was modeled with linear profiles. In the fitted profiles (curves c and e) this interface is smeared out. Furthermore, after the second annealing (curve e) we observe an enrichment of the deuterated PMMA at the polymer–air interface. The thickness of the PMMA (D) layer changed from 51.2 to 49.6 nm during annealing and the thickness of the PVC (H) layer increased from 49.6 to 51.3 nm. The interface width of the polymer–polymer interface is about 6 nm. The thickness of the enrichment layer is approximately 4 nm.

profile. Profiles consisting of  $N = 64$  layers were used in fits of the data with the simulated annealing procedure. The fit to the sample annealed for 3.5 h was performed with  $p = 0.01$ ,  $C = 0.5 \times 10^{-6}$  and a probability for the change of thicknesses of 0.5%. After 60 iterations a smoothing of the whole curve except the polymer–air interface was performed. After further 30 iterations followed by smoothing and another 15 iterations, the result shown in Figure 3c is reached. The fit to the reflectivity curve of the sample annealed for 7.5 h was performed in a similar manner with  $C = 0.5 \times 10^{-6}$ ,  $p = 0.01$  and a probability of changing a layer thickness of 1%. It took a total of 260 iterations. The polymer–air interface could not be kept constant in this case since otherwise it was not possible to obtain a good fit. Typical computation times for those fits were 15 min. It is not reasonable to increase the number of steps or the number of iterations since the fits already show very good agreement with experimental data within statistical errors. In both fits the linear starting profile is smeared out approaching an error-function-type profile. The exact analytical form is difficult to analyze.

A striking feature of the sample with longer annealing time is the enrichment of deuterated PMMA at the air–polymer interface. This can be understood from a lower

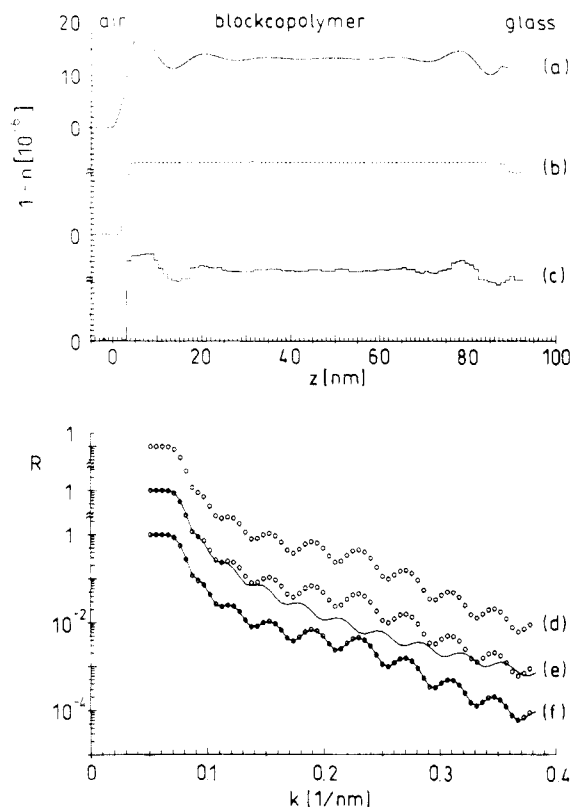


**Figure 4.** Neutron scattering density profiles given by  $(1 - n)$  for a polystyrene/butadiene diblock copolymer and corresponding reflectivity curves: (a) model profile used to generate calculated reflectivity curves for further fits ( $L = 14.3$  nm,  $\xi = 8.9$  nm); (b) starting profile for fit; (c) final fitted profile from simulated annealing fits. Corresponding reflection curves are also given (d–f). The starting profile for the fit, curve b, and the corresponding reflectivity curve, curve e, does not describe the data well, while the fitted profile, curves c and f, both reproduce the model reflectivity data and the model profile quite well.

surface tension of PMMA with respect to PVC and a diffusion of PMMA through the relatively thick PVC layer. Small PMMA concentrations in the PVC layer are difficult to detect with neutron reflectometry since the PVC level in the  $(1 - n)$  plot will only change slightly. The reflectivity curve is not very sensitive on the exact location of this level. Surface enrichment in a blend of deuterated and protonated polystyrene has been observed previously by neutron reflectometry.<sup>39</sup> This example of PMMA/PVC interdiffusion is a nice demonstration that a model-free fit to reflectivity data can reveal specific features of the scattering density profile which one might not initially tend to include in a simple analytic fitting procedure.

In the following we will illuminate some of the problems connected with model-free fits to reflectivity data. We will first discuss variations of the fitting algorithm on the results, show the influence of starting parameters and profiles on a reasonable fit, and finally discuss relevant parameters of the simulated annealing procedure. We use another example of a model profile describing surface-induced order in block copolymers as expressed theoretically by Fredrickson.<sup>40</sup> Also experimentally surface-induced order in block copolymers has been investigated<sup>41,42</sup> originating from the surface enrichment of one component due to a lower surface tension. A typical profile is shown in Figure 4a for a diblock copolymer with one block deuterated. Data correspond to a symmetric diblock copolymer of polystyrene and polybutadiene of total molecular weight 34 000. Theory<sup>40</sup> predicts an exponentially damped cosine modulation of period  $L$  and correlation length  $\xi$ . For the following fits the reflectivity curve

calculated from this profile, Figure 4d, is taken as the "experimental" curve.

For a simulated annealing fit one may assume a constant mean scattering density over the film, Figure 4b, as a starting profile. The corresponding reflectivity curve, the solid line in Figure 4e, shows significant deviations from the target curve. The result of the fit, Figure 4c, reveals all the relevant features of the model profile and yields an excellent fit of the model reflectivity data, Figure 4f. One might, however, ask the question how significant such a fit really is and whether there are not other possibilities to interpret the given reflectivity curve, Figure 4d. We will try to illuminate this question which actually has to be put for most scattering investigations in a similar way, from various viewpoints.

First we can ask, how much the used algorithm influences the result. We checked three different algorithms for the acceptance of changes in the profile. In all cases the change is accepted if  $F_n < F_{n-1}$ ; otherwise the change is accepted only with the probability

- (1)  $p = \text{constant}$
- (2)  $p = \exp\left(\frac{F_0 - F_n}{T}\right)$
- (3)  $p = \exp\left(\frac{(F_0 - F_n)}{F_n} \frac{1}{T}\right)$

Case 1 used for values of  $p$  between 0.05 and 0.0001 reveals usually quite fast converging fits, which are, however, still able to escape from local minima. The final fits are not sensible to the exact value of  $p$ . The fits presented here are obtained with values of the  $p = 0.001$ .

Case 2 proves to be very sensitive in choosing the right analogue temperature  $T$ . If  $T$  is taken too small, the fit will be captured in a local minimum, if it is too great the fit will be quite noisy before being good. Furthermore it is necessary to lower the temperature  $T$  during the fit to obtain good results. So we did not use this case for any of the fits presented here. Case 3 is also rather insensitive on the "temperature"  $T$  and converges even better than case 1 if  $T$  is set to about 0.002.

Figure 5 shows fits done with algorithms 1 and 3. Several profiles in different stages of the fit are plotted over one another. Both procedures yield rather good fits and produce similar profiles in different runs. The fits using algorithm 3 are slightly better and exhibit smaller differences among each other. Fits using algorithm 1 with  $p = 0.01$  and with algorithm 3 with  $T = 0.002$  find the same minimal  $F$  values. Both leave local minima with similar probabilities, but algorithm 3 explores these minima in more detail and recovers faster after an escape of local minima. All other examples presented here are calculated with algorithm 3 and  $T = 0.002$ .

In Figure 6 fits obtained from constant starting profiles with different mean  $n$  are shown. If the mean  $n$  value of the starting profile, case b ( $1 - n = 1.35 \times 10^{-5}$ ), coincides with the model profile to be fitted (Figure 6b) the fit converges rather fast (400 iterations, 40 min CPU time,  $F = 0.01$ ) and is in best agreement with the model data. If  $n$  of the starting profile deviates from the mean  $n$  of the model profile to be fitted (a)  $1 - n = 1.75 \times 10^{-5}$  or (c)  $1 - n = 1.0 \times 10^{-5}$ , which corresponds to the changes in  $\phi$  of  $\pm 0.2$ , the fit needs much more computing time to converge and the best fit is not as good as in case b mentioned above (1000–2000 iterations to obtain values (a) of  $F = 0.08$  in 100 min or (c)  $F = 0.33$  in 200 min). Nevertheless all fits show a surface-induced order with the right periodicity  $L$  and decay length  $\xi$  in the sample.

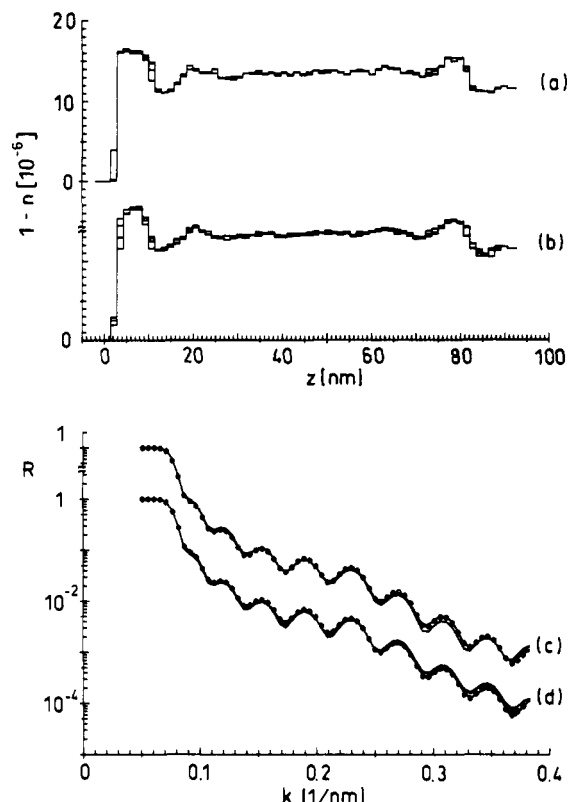


**Figure 5.** A comparison of fits obtained by algorithm 1 (curves b and d) and 3 (curves a and c) as explained in the text. Several fitted profiles at different annealing stages during the fit are plotted one over another (between 400 and 1000 iterations). The reflectivity data are reproduced by both fitting algorithms, but fits with algorithm 3 converge slightly better than those with algorithm 1.

If the  $n$  values of the starting profiles differ even more than in the cases shown, the simulated annealing fits fail to converge to a reasonable agreement with the reflectivity data.

In all the above cases the layer thickness in the starting profile was not equidistant but with a greater density of layers in the region where surface induced order was expected and changes in  $n$  should have been greatest. A fit with equidistant distributed layers converges in about the same time (ca. 400 iterations, case b above) and fitted profiles do not differ significantly. The nonequidistant distribution of layers leads to better  $F$  values since the given structure can be better approximated. A final check concerns the smoothing procedure at different stages of the simulated annealing fit.

As already mentioned before in section 2, one needs to put certain precautions concerning the smoothness onto the fitted profile. Otherwise one would obtain profiles with small scale oscillations which are of no physical significance. The constraint parameter ( $C$ ) turns out to be a rather important parameter in the fits. If  $C < 10^{-6}$ , the fit will converge only very slowly if it converges at all. Choosing values of  $C > 10^{-6}$  the fit will converge very fast but will lead to profiles with rather strong short range oscillations. Figure 7 gives an example where  $C$  was set to  $2.5 \times 10^{-6}$  instead of  $0.5 \times 10^{-6}$  used for all other calculations. This fit was obtained in only 10 iterations (5 min of CPU time) and yields an  $F$  value of 0.77. Smoothing the profile will still give a reasonable fit with  $F = 2.2$  (Figure 7b). Of course, there are deviations from the data both before and after smoothing of the profile, but repeated fitting and smoothing will improve the fit and is on the other hand a very fast way to get an idea what the profile might look like.



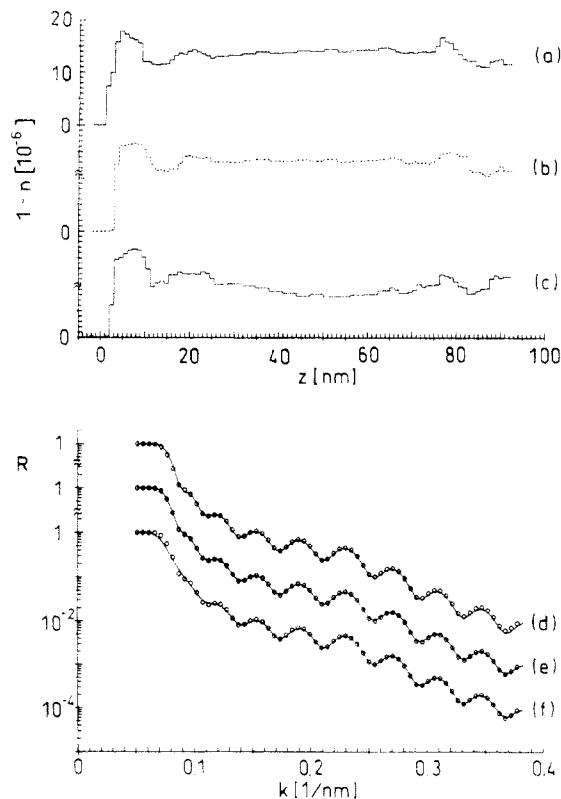


**Figure 6.** Fits obtained from different starting profiles with varying mean scattering density, (a)  $1 - n = 1.75 \times 10^{-6}$ ; (b)  $1 - n = 1.35 \times 10^{-6}$ ; (c)  $1 - n = 1.0 \times 10^{-6}$ , and corresponding reflectivity curves (d-f). All fits describe model reflectivity data quite well. The profiles exhibit the major features of the model profile shown in Figure 4a. The fit starting with the correct mean  $n$  (curve b) results in the best profile and fit (curve e).

#### 4. Conclusion

We have shown in several examples, which include both calculated as well as experimental neutron reflectivity curves, that the technique of simulated annealing in connection with the matrix technique provides a versatile tool to obtain density profiles from reflectivity data. With minimal knowledge about the system to construct a reasonable starting profile for the fit, one can obtain a model-free solution to this ill-posed problem. The principal problem is that one generally is lacking knowledge about phases during the inverse Fourier transform which results in multiple minima and ambiguities for the solution. With additional information about the sample, one can try to overcome this problem. The proposed simulated annealing technique thus uses the knowledge about the sample in an optimal way and has been adapted by some modifications to the complex problem of fitting neutron reflectivity data. It may, however, not be considered to be a mathematically unique and strict procedure.

A modified computational technique has been proposed utilizing a matrix tree algorithm. This technique may be generally used in similar problems and can significantly reduce computation time during fits. Depending on complexity of the fit and quality of the starting profile, reasonable computing times are needed and the technique may well be used as a "standard" procedure for the analysis of reflectivity data. For comparison with theory or quantitative analysis an additional fit of reflectivity data with a particular model might still be necessary, but simulated annealing can considerably help in the construction of such an analytic model which is otherwise sometimes difficult to obtain. Techniques of this sort will be needed to provide a solid basis for data analysis of

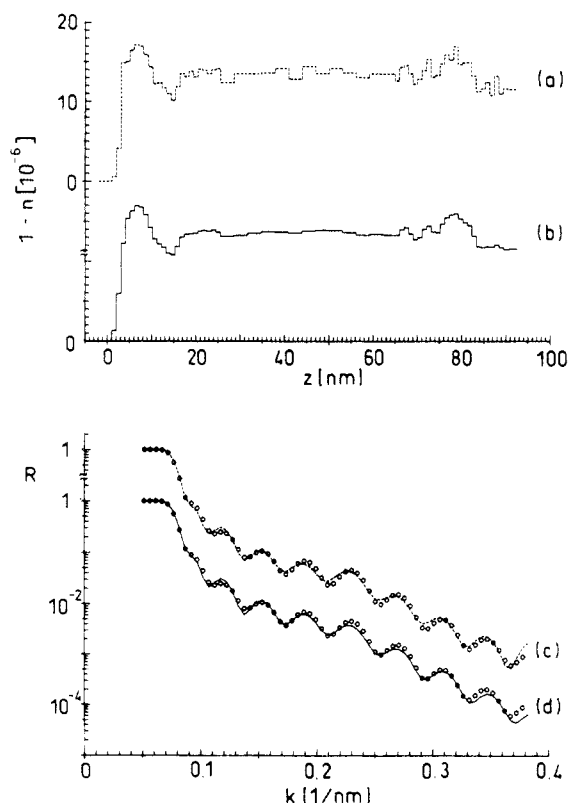


**Figure 7.** Effect of smoothing procedures on simulated annealing fits: Relaxed constraints ( $C = 2.5 \times 10^{-6}$ ) (curves a and c) on the smoothness of the profile lead to a very fast convergence of the fit but a profile with strong short range oscillations. Smoothing over these oscillations (curves b and d) gives a smooth profile which still approximates the model profile (Figure 4a) reasonably well.

reflectivity data which can be otherwise quite time-consuming. With the increasing number of neutron reflectometers and thus also the increasing number of users of this technique, standard procedures of data analysis will be needed.

The technique can of course equally well and with only minor modifications be applied to X-ray reflectivity data. Here, however, one is faced with the contrast problem which in the case of X-rays and polymers is much more difficult to resolve as compared to the neutron case where a suitable contrast between components can be generally achieved by deuteration.

**Acknowledgment.** We acknowledge very helpful discussions with Dr. G. Reiter and technical help of B. Derichs during the neutron reflectivity experiments. Neutron measurements were performed at Forschungsanlage Jülich in the framework of a cooperation agreement with the Max-Planck-Institute and were supported by a research grant from BMFT.

#### References and Notes

- (1) Russell, T. P. *Mater. Sci. Rep.* **1990**, *5*, 171.
- (2) Stamm, M.; Reiter, G.; Kunz, K. *Physica B* **1991**, *173*, 35.
- (3) Stamm, M. *Adv. Polym. Sci.* **1992**, *100*, 357.
- (4) Karim, A.; Mansour, A.; Felcher, G. P.; Russell, T. P. *Phys. Rev. B* **1990**, *42*, 6846.
- (5) Stamm, M.; Hüttenbach, S.; Reiter, G.; Springer, T. *Europhys. Lett.* **1991**, *14*, 451.
- (6) Jones, R. A. L.; Norton, L. J.; Kramer, E. J.; Composto, R. J.; Stein, R. S.; Russell, T. P.; Mansour, A.; Karim, A.; Felcher, G. P.; Rafailovich, M. H.; Sokolov, J.; Zhao, X.; Schwarz, S. A. *Europhys. Lett.* **1990**, *12*, 41.

- (7) Russell, T. P.; Menelle, A.; Anastasiadis, S. H.; Satija, S. K.; Majkrzak, C. F. *Macromolecules* **1991**, *24*, 6263.
- (8) Kirkpatrick, S.; Gelatt, C. O.; Vecchi, M. P. *Science* **1983**, *220*, 671.
- (9) Pannetier, J. In *Neutron Scattering Data Analysis*; Johnson, M. W., Ed.; Institute of Physics Conference Series; American Institute of Physics: New York, 1990; Vol. 107; p 213.
- (10) Lekner, J. *Theory of Reflection*; Martinus Nijhoff Publishing: Dordrecht, 1987.
- (11) Abelès, F. *Ann. Phys. (Paris)* **1950**, *12*, 596.
- (12) Parratt, L. G. *Phys. Rev.* **1954**, *95*, 359.
- (13) Ankner, J. F. In *Surface X-ray and Neutron Scattering*; Zabel, H., Robinson, I. K., Eds.; Springer Proceedings in Physics; Springer: Berlin, 1992; Vol. 61, p 105.
- (14) Lekner, J. *Physica B* **1991**, *173*, 99.
- (15) Sinha, S. K.; Sirota, E. B.; Garoff, S.; Stanelly, H. B. *Phys. Rev. B* **1988**, *38*, 2297.
- (16) Pershan, P. S.; Braslau, A.; Weiss, A. H.; Als-Nielsen, J. *Phys. Rev. A* **1987**, *15*, 4800.
- (17) Felcher, G. P.; Dozier, W. D.; Huang, Y. Y.; Zhou, X. L. In *Surface X-ray and Neutron Scattering*; Zabel, H., Robinson, I. K., Eds.; Springer Proceedings in Physics; Springer: Berlin, 1992; Vol. 61, p 99.
- (18) Crowley, T. L.; Lee, E. M.; Simister, E. A.; Thomas, R. K. *Physica B* **1991**, *173*, 143.
- (19) Penfold, J.; Thomas, R. K. *J. Phys. Cond. Mat.* **1990**, *2*, 1369.
- (20) Zhou, X. L.; Felcher, G. P.; Chen, S. H. *Physica B* **1991**, *173*, 167.
- (21) Tidswell, I. M.; Ocko, B. M.; Pershan, P. S.; Wassermann, S. R.; Whitesides, G. M.; Axe, J. D. *Phys. Rev. B* **1990**, *41*, 1111.
- (22) Toney, M. F.; Thompson, C. J. *Chem. Phys.* **1990**, *92*, 3781.
- (23) Sinha, S. K.; Sanyal, M. K.; Huang, K. G.; Gibaud, A.; Rafailovich, M.; Sokolov, J.; Zhao, X.; Zhao, W. In *Surface X-ray and Neutron Scattering*; Zabel, H., Robinson, I. K., Eds.; Springer Proceedings in Physics; Springer: Berlin, 1992; Vol. 61, p 85.
- (24) Sanyal, M. K.; Sinha, S. K.; Gibaud, A.; Huang, K. G.; Carvalho, B. L.; Rafailovich, M.; Sokolov, J.; Zhao, X.; Zhao, W., submitted for publication.
- (25) Dozier, W. D.; Carpenter, J. M.; Felcher, G. P. *Bull. Am. Phys. Soc.* **1991**, *36*, 772.
- (26) Pederson, J. S., submitted for publication.
- (27) Worcester, D. L. *Physica B* **1991**, *173*, 139.
- (28) Pederson, J. S. Private communication.
- (29) Sivia, D. S.; Hamilton, W. A.; Smith, G. S. *Physica B* **1991**, *173*, 121.
- (30) Laarhoven, P. J. M.; Aarts, E. H. L., Eds. *Simulated Annealing: Theory and Applications*; Dordrecht, Reidel, 1987.
- (31) Johnson, M. E. *Am. J. Math. Manage. Sci.* **1988**, *8*, 205.
- (32) Brünger, A. T. *Annu. Rev. Phys. Chem.* **1991**, *42*, 197.
- (33) Zhang, H.; Wool, R. P. *ACS Polym. Prepr.* **1990**, *31*, 511.
- (34) Reiter, G.; Steiner, U. *J. Phys. II* **1991**, *1*, 659.
- (35) Stamm, M. In *The Physics of Polymer Surfaces and Interfaces*; Sanchez, I. C., Ed.; Butterworth-Heinemann: Boston, MA 1992; p 163.
- (36) de Gennes, P. G. In *The Physics of Polymer Surfaces and Interfaces*; Sanchez, I. C., Ed.; Butterworth-Heinemann: Boston, MA, 1992; p 55.
- (37) Foster, M.; Stamm, M.; Reiter, G.; Hüttenbach, S. *Vacuum* **1990**, *41*, 1441.
- (38) Jäger, H.; Vorenkamp, E. J.; Challa, G. *Polym. Commun.* **1983**, *24*, 290.
- (39) Jones, R. A. L.; Norton, L. J.; Kramer, E. J.; Composto, R. J.; Stein, R. S.; Russell, T. P.; Mansour, A.; Karim, A.; Felcher, G. P.; Rafailovich, M. H.; Sokolov, J.; Zhao, X.; Schwarz, S. A. *Europhys. Lett.* **1990**, *12*, 41.
- (40) Fredrickson, G. H. *Macromolecules* **1987**, *20*, 2535.
- (41) Menelle, A.; Russell, T. P.; Anastasiadis, S. H.; Satija, S. K.; Majkrzak, C. F. *Phys. Rev. Lett.* **1992**, *68*, 67.
- (42) Stamm, M.; Götzelmann, A.; Geissler, K. H.; Rauch, F. *Prog. Colloid Polym. Sci.* **1993**, *91*, 101.